Institute of Paper Science and Technology
Atlanta, Georgia

IPST Technical Paper Series Number 851

A Micromechanically Based Couple-Stress Model of an Elastic Two-Phase Composite

F. Bouyge, I. Jasiuk, and M. Ostoja-Starzewski

May 2000

Submitted to
International Journal of Solids and Structures
Mechanics Pan-America 2000
(Special Issue)

INSTITUTE OF PAPER SCIENCE AND TECHNOLOGY
PURPOSE AND MISSIONS

The Institute of Paper Science and Technology is an independent graduate school, research organization, and information center for science and technology mainly concerned with manufacture and uses of pulp, paper, paperboard, and other forest products and byproducts. Established in 1929 as the Institute of Paper Chemistry, the Institute provides research and information services to the wood, fiber, and allied industries in a unique partnership between education and business. The Institute is supported by 52 North American companies. The purpose of the Institute is fulfilled through four missions, which are:

- to provide multidisciplinary graduate education to students who advance the science and technology of the industry and who rise into leadership positions within the industry;
- to conduct and foster research that creates knowledge to satisfy the technological needs of the industry;
- to provide the information, expertise, and interactive learning that enables customers to improve job knowledge and business performance;
- to aggressively seek out technological opportunities and facilitate the transfer and implementation of those technologies in collaboration with industry partners.

ACCREDITATION

The Institute of Paper Science and Technology is accredited by the Commission on Colleges of the Southern Association of Colleges and Schools to award the Master of Science and Doctor of Philosophy degrees.

NOTICE AND DISCLAIMER

The Institute of Paper Science and Technology (IPST) has provided a high standard of professional service and has put forth its best efforts within the time and funds available for this project. The information and conclusions are advisory and are intended only for internal use by any company who may receive this report. Each company must decide for itself the best approach to solving any problems it may have and how, or whether, this reported information should be considered in its approach.

IPST does not recommend particular products, procedures, materials, or service. These are included only in the interest of completeness within a laboratory context and budgetary constraint. Actual products, materials, and services used may differ and are peculiar to the operations of each company.

In no event shall IPST or its employees and agents have any obligation or liability for damages including, but not limited to, consequential damages arising out of or in connection with any company's use of or inability to use the reported information. IPST provides no warranty or guaranty of results.

A micromechanically based couple-stress model of an elastic two-phase composite

Frederic Bouyge[1], Iwona Jasiuk[1] and Martin Ostoja-Starzewski[2]

[1]The George W. Woodruff School of Mechanical Engineering, Georgia Institute of Technology
Atlanta, GA 30332-0405, U.S.A.

[2]Institute of Paper Science and Technology, and Georgia Institute of Technology
500 10th Street, N.W., Atlanta, GA 30318-5794, U.S.A.

Abstract

The study reported in this paper concerns the determination of couple-stress moduli and characteristic lengths of heterogeneous materials. The study is set in the context of a planar (two-dimensional), two-phase composite with linear non-couple-stress (classical), elastic constituents, with a single microstructural length scale (inclusion spacing) in an equilateral triangular array. We use an approach which allows a replacement of this composite by an approximating couple-stress continuum. We determine the effective material parameters from the response of a unit cell under either displacement, displacement-periodic, or traction boundary conditions. We carry out computations of all the moduli by varying the stiffness ratio of both phases, so as to cover a range of very different materials from porous solids through composites with rigid inclusions. It is found that the three boundary conditions result in hierarchies of couple-stress moduli. In addition, we observe from our numerical computations that these three boundary conditions also result in a hierarchy of characteristic lengths.

---

to be published in

Intl. Journal of Solids and Structures (Special Issue: *Mechanics Pan-America 2000*)

1. INTRODUCTION

Classical continuum theories show discrepancies with experiments when a material microstructure gives rise to sharp gradients of dependent fields. Cosserat-type (or microcontinuum-type) theories, dating back to the Cosserat brothers (Cosserat, 1909), attempt to account for these phenomena. Although a number of theoretical results have been obtained, the full utility of Cosserat-type theories hinges on one's ability to determine the constitutive coefficients. Indeed, some progress in that direction has been made over the past three decades, but the situation is still one of theoreticians being well ahead of the experimentally available results (e.g., Nowacki, 1986). The work we report here aims at remedying the situation through micromechanical analysis rather than the experiment.

It appears that, in general, the issue of determination of micropolar coefficients has been addressed in four types of problems: (a) crystal lattice systems (Askar, 1986); (b) regular beam networks [e.g., Wozniak (1970); Bazant and Christensen (1972)]; (c) laminated composites [e.g., Herrmann and Achenbach (1968)]; and (d) granular media and foams [e.g., Perkins and Thomson (1973), Lakes (1983, 1986, 1995), Yang and Lakes (1982)]. All these systems have one feature in common: they exhibit some definite microstructure, which, as is well known, forms the motivation of all the investigations of Cosserat-type models and theories.

Thus, works in the first and second category start out with a very clearly set periodic system of particles interacting via forces and moments modeled by either interatomic potentials or beams. Laminated composites offer a quite similar advantage thanks to their clearly defined geometry. The situation with foams and granular media is more difficult due to a spatially disordered geometry of those materials - and therefore, they have principally been studied through experiments.

In a recent study, Forest and Sab (1998) proposed a methodology for derivation of an effective, homogeneous Cosserat-type continuum for a heterogeneous Cauchy-type continuum. Their approach is an extension of the classical homogenization method [e.g., Sanchez-Palencia and Zaoui (1987)] - it hinges on a representation of the macroscopic displacement field by a polynomial main field and a periodic perturbation. More specifically, they show three levels of the polynomial expansion: (i) the linear one leads to a classical Cauchy-type continuum, (ii) the quadratic one leads to a couple-stress continuum, also called a *restricted model* by Nowacki (1986), and (iii) the third-order one (respectively, fourth order in three dimensions) leads to an unrestricted Cosserat-type (micropolar) continuum. Using a finite element method, Forest and Sab also demonstrate the def-

inite advantage of replacing the actual Cauchy-type microstructure by the Cosserat-type continuum: a much smaller number of degrees of freedom is required in the homogenized model.

Model of type (ii) has recently been pursued by Ostoja-Starzewski *et al.* (1999). We carried out that study in the context of a planar, periodic, effectively isotropic, two-phase composite with linear elastic constituents of classical Cauchy-type, with a microstructural length scale given by the inclusion spacing. We subjected the unit cell to periodic boundary conditions. In the limit of very low stiffness of the inclusion phase we have obtained moduli that showed very good agreement with analytical derivations of beam-framework models (Wozniak, 1970). Of additional interest to us was the determination of the somewhat enigmatic characteristic length l - a parameter apparently first introduced in the analytical studies in the sixties, when it showed up in the elastostatic field equations. While in the past, l was postulated to be equal to the average cell or grain size, with all the moduli in hand we could now easily compute l, and, in fact, found it to be a fraction of the microstructural cell size - from about one tenth to fourth of it - for composites of the type described at the top of this paragraph at volume fractions from 3.6%-58%.

In this paper we continue this initial study by considering couple-stress moduli and characteristic lengths of the above described composite under several additional types of boundary conditions: displacement, displacement-periodic, and traction boundary conditions. We then find that these boundary conditions result in hierarchies of couple-stress moduli. The motivation of this paper lies in the fact that we cannot apply periodic boundary conditions in one of the tests (the bending test). Thus, we use an alternate approach involving displacement and traction boundary conditions to obtain bounds on couple-stress moduli and compare those with periodic and displacement-periodic boundary condition results. This investigation complements our other studies of boundary condition effects on elastic moduli of composites, e.g. Jiang *et al.* (2000).

2. PROBLEM FORMULATION

The leitmotif of this paper is to replace a complex microstructure by a higher-order (i.e., Cosserat) continuum. Once done, this allows one to work with a homogeneous material model, yet endowed with one extra degree of freedom - that of rotation. In this paper we address the issue of effective couple-stress moduli in the context of linear elastic microstructures with a single microstructural length scale such as the mean inclusion spacing. In particular, we remove the aspect of geometric disorder by focusing on a periodic composite material with an equilateral, triangular

arrangement of circular inclusions. This geometry gives us a composite material which is effectively isotropic. We take the periodic unit cell as a rhombus-shaped domain of edge length L and volume $V = bL^2\sqrt{3}/2$, Fig. 1. The rhombus' height in the x_2 direction is $H = 2h = L\sqrt{3}/2$, and its thickness in the x_3 is b.

The inclusion (i) and matrix (m) phases follow classical (linear elastic, isotropic) elasticity; they have Young's moduli E^i and E^m, and Poisson's ratios ν^i and ν^m, respectively. By varying the stiffness ratio E^i/E^m we can model a wide range of materials with either stiff or soft inclusions, and in the extreme cases of this ratio tending to either ∞ or 0, we approach composites with rigid inclusions or pores. It is important to note, however, that the special case of no mismatch ($E^i/E^m = 1$) implies no microstructure, so the couple stress model becomes unnecessary in that special case.

We focus here on the first planar problem of Cosserat elasticity (Nowacki, 1986) with displacement $\boldsymbol{u} = (u_1, u_2, 0)$ and rotation $\varphi = (0, 0, \varphi_3)$; this is a generalization of the classical in-plane elasticity, and consider a couple-stress (or, restricted continuum) model, in which rotation depends on displacement gradients in the same manner as in classical elasticity. The kinematics of the body is described by u_1, u_2, and $\varphi_3 = (u_{2,1} - u_{1,2})/2$, which define the strain tensor γ_{ij} and the (bending) curvature tensor κ_{i3}, $i, j = 1, 2$. The force field is specified by force-stress tensor τ_{ij} and couple-stress tensor μ_{i3}, $i, j = 1, 2$.

The composite of Fig. 1 is centrosymmetric: there is no coupling between τ_{ij} and κ_{i3} on one hand and between γ_{ij} and μ_{i3} on the other. Thus, the constitutive law will involve two stiffness tensors $C^{(1)}_{ijkl}$ and $C^{(2)}_{i3k3}$ only, which are defined via

$$\tau_{ij} = C^{(1)}_{ijkl}\gamma_{kl} \qquad \mu_{i3} = C^{(2)}_{i3k3}\kappa_{k3} \qquad i, j, k, l = 1, 2 \tag{1}$$

Equivalently, we can work with their inverses: compliances $S^{(1)}_{ijkl}$ and $S^{(2)}_{i3k3}$. In the isotropic case,

the latter are

$$S^{(1)}_{ijkl} = \frac{1}{4}[S(\delta_{ik}\delta_{jl} + \delta_{il}\delta_{jk}) + (A - S)\delta_{ij}\delta_{kl}] \qquad S^{(2)}_{i3k3} = \delta_{ik}M \tag{2}$$

where A, M and S are three independent planar couple-stress constants defined in (Ostoja-Starzewski and Jasiuk, 1995).

Note that A and S are the area bulk compliance and shear compliance, respectively, and they are the same as in classical plane elasticity. M is the additional independent constant, which has a dimension differing from A and S by length squared. This gives rise to a length scale present in the couple-stress theory (a special case of the Cosserat theory), which is absent in the classical elasticity theory. This length is quantitatively grasped by a characteristic length l defined as

$$l = \sqrt{\frac{S}{4M}} = \sqrt{\frac{S^{(1)}_{1212}}{S^{(2)}_{1313}}} \tag{3}$$

In this paper we obtain the effective response of composites by employing the couple-stress theory, which therefore gives the second constitutive tensor $C^{(2)}_{i3k3}$ (in addition to $C^{(1)}_{ijkl}$ present in classical theory), which captures the information on the microstructure. This information is *not* captured by classical micromechanics approaches for predictions of effective elastic moduli of heterogeneous materials.

Note that the unit cell's response under non-periodic boundary conditions is anisotropic, but the departure from isotropy is on the order of only a few percent for the composite systems with inclusion volume fraction of 18% studied in this paper. This makes an approximate comparison of stiffness tensors (both $C^{(1)}_{ijkl}$ and $C^{(2)}_{ijkl}$) found from non-periodic boundary conditions (this paper) with those from periodic ones (previous paper) possible. Additionally, this allows a discussion of all the results in the context of an isotropic material model.

3. BOUNDARY CONDITIONS ON THE UNIT CELL

The main goal of our analysis is the determination of effective constitutive coefficients from the unit cell response of a two-phase composite described in Section 2. We consider three types of boundary conditions for determination of the effective couple-stress moduli for a material domain

B having boundary ∂B (Fig. 1): (i) displacement; (ii) displacement-periodic; and (iii) traction. In each case we compute, by a finite element method, the total elastic strain energy stored in the unit cell of the two-phase composite U^{cell} (= U^{*cell}) as a functional of Cauchy strains ε_{ij} (respectively, Cauchy stresses σ_{ij}). Separately, for the first two boundary conditions, we set up the energy $U^{couple-stress}$ corresponding to an effective, homogeneous couple-stress continuum, which is a functional of the strains γ_{ij} and the curvatures κ_{i3}. By setting

$$U^{couple-stress} = U^{cell} \tag{4}$$

we then infer the effective stiffness tensors $C^{(1)}_{ijkl}$ and $C^{(2)}_{i3k3}$. On the other hand, in the case of traction boundary conditions, we work with the complementary energy $U^{*couple-stress}$ - a functional of τ_{ij} and μ_{i3} - and, from

$$U^{*couple-stress} = U^{*cell} \tag{4'}$$

we then obtain the effective compliance tensors $S^{(1)}_{ijkl}$ and $S^{(2)}_{i3k3}$.

Displacement boundary conditions. The total elastic strain energy stored in the unit cell is

$$U^{cell} = \frac{1}{2}\int_V \varepsilon_{ij} C_{ijkl} \varepsilon_{kl} dV \tag{5}$$

while that of an approximating couple-stress continuum involves, in general, two terms

$$U^{couple-stress} = \frac{V}{2}[\gamma_{ij} C^{(1)}_{ijkl} \gamma_{kl} + \kappa_{i3} C^{(2)}_{i3k3} \kappa_{k3}] \tag{6}$$

where γ_{ij} in (6) stands for the effective strain of the unit cell in the couple-stress continuum and κ_{i3} is the effective curvature; V is the volume of the unit cell B defined in Section 2. To determine $C^{(1)}_{ijkl}$ we conduct two tests:

(i) Uniaxial extension

If we apply γ_{22} the displacement boundary conditions become

$$u_1(\boldsymbol{x}) = 0 \qquad u_2(\boldsymbol{x}) = \gamma_{22}x_2 \qquad \forall \boldsymbol{x} \in \partial B \tag{7}$$

which yields $C^{(1)}_{2222} = 2U^{cell}/V$ when we set $\gamma_{22} = 1$; alternately, we could apply $u_1(\boldsymbol{x}) = \gamma_{11}x_1$ and $u_2(\boldsymbol{x}) = 0$, which would yield $C^{(1)}_{1111}$. For our composite, $C^{(1)}_{1111}$ is approximately (within 5 %) equal to $C^{(1)}_{2222}$ for all the stiffness mismatches considered.

(ii) Simple shear

$$u_1(\boldsymbol{x}) = \gamma_{12}x_2 \qquad u_2(\boldsymbol{x}) = 0 \qquad \forall \boldsymbol{x} \in \partial B \tag{8}$$

which yields $C^{(1)}_{1212} = 2U^{cell}/V$ when we set $\gamma_{12} = 1$. There are two more possibilities here: either apply $u_1(\boldsymbol{x}) = 0$ and $u_2(\boldsymbol{x}) = \gamma_{12}x_1$, or $u_1(\boldsymbol{x}) = \gamma_{12}x_2/2$ and $u_2(\boldsymbol{x}) = \gamma_{12}x_1/2$. Finally, to determine $C^{(2)}_{i3k3}$, we conduct

(iii) Bending test

$$u_1(\boldsymbol{x}) = -x_1x_2\kappa_{13} \qquad u_2(\boldsymbol{x}) = \frac{x_1^2}{2}\kappa_{13} \qquad \forall \boldsymbol{x} \in \partial B \tag{9}$$

We note that γ_{ij} in equation (6) may be zero or non-zero, depending on the coordinate system chosen. For the bending test, the only possible non-zero strain component is $\gamma_{11} = \int_V u_{1,1}dV/V = \int_{\partial B} u_1 n_1 dS/V$. When we take the origin of coordinates at the rhombus corner, (9) yields the average strain in the couple-stress medium $\gamma_{11} = -h\kappa_{13}$, which results in $C^{(2)}_{1313} = 2U^{cell}/V - h^2C^{(1)}_{1111}$, whereby (recall (4)) $U^{cell} = U^{couple-stress} = V[\gamma_{11}C^{(1)}_{1111}\gamma_{11} + \kappa_{13}C^{(2)}_{1313}\kappa_{13}]/2$. When the origin of the coordinate system is at the cell's center, then $\gamma_{11} = 0$, and thus the term involving $C^{(1)}_{1111}$ in the latter expression vanishes. Also here there exists another possibility for carrying the bending test: $u_1(\boldsymbol{x}) = x_2^2\kappa_{23}/2$ and

$u_2(x) = -x_1 x_2 \kappa_{23}$. This test would yield $C^{(2)}_{2323}$, which, for our study, is only approximately equal to $C^{(2)}_{1313}$, given the anisotropy issue mentioned earlier.

The deformation modes for the above three tests under displacement boundary conditions are shown in Fig. 2. Note that in the last test (bending test) the coordinate system's origin is chosen at the lower left corner.

Displacement-periodic conditions. The energies U^{cell} and $U^{couple-stress}$ are given by (5) and (6), respectively. Here we choose to apply the displacement boundary conditions on the two horizontal boundaries of the rhombus ∂B_d, and the periodic boundary conditions on the remaining slanted boundaries $\partial B_p = \partial B - \partial B_d$. To determine $C^{(1)}_{ijkl}$ we conduct two tests.

(i) Uniaxial extension

If we apply γ_{22}, the periodic boundary conditions are given by

$$u_i(x + Le_1) = u_i(x) \qquad t_i(x + Le_1) = -t_i(x) \qquad \forall x \in \partial B_p \tag{10}$$

and the displacement boundary conditions are given by (7) on ∂B_d; e_1 is the unit vector along x_1. Thus, the controlled uniaxial extension $\gamma_{22} = 1$ yields $C^{(1)}_{2222} = 2U^{cell}/V$. Of course, alternately, we could apply γ_{11} so that the periodic boundary conditions on slanted faces would take the form $u_i(x + Le_1) = u_i(x) + \gamma_{11} Le_1$ and $t_i(x + Le_1) = -t_i(x)$, while the displacement boundary conditions on horizontal faces would be $u_i(x) = \gamma_{11} x_1$ and $u_2(x) = 0$.

(ii) Simple shear γ_{12}.

The periodic boundary conditions are given by

$$\begin{aligned} u_i(x + Le_1) &= u_i(x) \qquad u_2(x + Le_1) = u_2(x) + \gamma_{12} Le_1 \\ & t_i(x + Le_1) = -t_i(x) \end{aligned} \qquad \forall x \in \partial B_p \tag{11}$$

and the displacement boundary conditions by

$$u_1(x) = \gamma_{12} x_2 \qquad u_2(x) = 0 \qquad \forall x \in \partial B_d \tag{12}$$

This yields $C^{(1)}_{1212} = 2U^{cell}/V$ (when we set $\gamma_{12} = 1$).

(iii) Bending test.

The periodic boundary conditions are given by

$$u_1(x + Le_1) = u_1(x) - x_1 x_2 \kappa_{13}\Big|_{x_1 = L|e_1|} = u_1(x) - Lx_2\kappa_{13}$$

$$u_2(x + Le_1) = u_2(x) - \frac{L^2}{2} x_1 \kappa_{13}\Big|_{x_1 = L|e_1|} \qquad \forall x \in \partial B_p \qquad (13)$$

$$t_i(x + Le_1) = -t_i(x)$$

while the displacement conditions on $\partial B_d = \partial B - \partial B_p$ are given by (9). Again, noting that $\gamma_{11} = \int_V u_{1,1} dV/V = \int_{\partial B} u_1 n_1 dS/V = -h\kappa_{13}$ if we take the origin of the coordinate system at the corner, this yields $C^{(2)}_{1313} = 2U^{cell}/V - C^{(1)}_{1111}$ in the same fashion as before.

The deformation modes for the above three tests under displacement-periodic boundary conditions are shown in Fig. 3, with the origin of the coordinate system being chosen at the rhombus' left corner.

In (Ostoja-Starzewski *et al.* 1999) we computed the $C^{(1)}_{ijkl}$ tensor under purely periodic boundary conditions, but the $C^{(2)}_{i3k3}$ tensor under displacement-periodic boundary conditions. The use of periodic boundary conditions applied to all surfaces for the evaluation of $C^{(1)}_{ijkl}$ is natural for a periodic microstructure considered and gives exact effective moduli. However, the test for the evaluation of $C^{(2)}_{i3k3}$, which involves bending, does not give a deformation which is periodic on horizontal faces of a rhombus-shaped unit cell. Thus, we could not use periodic boundary conditions on all surfaces, and have used displacement-periodic boundary conditions for bending test instead. For consistency, in the present computation we use the same boundary conditions (displacement-periodic) for both $C^{(1)}_{ijkl}$ and $C^{(2)}_{i3k3}$. In addition we use displacement (as described already) and traction conditions which bound periodic and displacement-periodic results.

Traction conditions. The total complementary energy stored in the unit cell is

$$U^{*cell} = \frac{1}{2}\int_V \sigma_{ij} S_{ijmn} \sigma_{mn} dV \tag{14}$$

while that of an approximating couple-stress continuum involves, in general, two terms

$$U^{*couple-stress} = \frac{V}{2}[\tau_{ij} S^{(1)}_{ijmn} \tau_{mn} + \mu_{i3} S^{(2)}_{i3k3} \mu_{k3}] \tag{15}$$

To determine $S^{(1)}_{ijkl}$ we conduct two tests:

(i) Uniaxial tension

$$t_1(\boldsymbol{x}) = \tau_{11} n_1 \qquad t_2(\boldsymbol{x}) = 0 \qquad \forall \boldsymbol{x} \in \partial B \tag{16}$$

which yields $S^{(1)}_{1111} = 2U^{*cell}/V$ (when we set $\tau_{11} = 1$). Application of the τ_{22} loading (to get $S^{(1)}_{2222}$) is unwieldy because of the unbalanced moment imposed by this loading.

(ii) Simple shear traction

$$t_1(\boldsymbol{x}) = \tau_{12} n_1 \qquad t_2(\boldsymbol{x}) = \tau_{12} n_2 \qquad \forall \boldsymbol{x} \in \partial B \tag{17}$$

which yields $S^{(1)}_{1212} = 2U^{*cell}/V$ (when we set $\tau_{12} = 1$. Finally, we conduct

(iii) Bending test:

$$t_1(\boldsymbol{x}) = \sigma_{11} n_1 = c x_2 n_1 \qquad t_2(\boldsymbol{x}) = 0 \qquad \forall \boldsymbol{x} \in \partial B \tag{18}$$

where $c = M_B/I$ (M_B being the bending moment and $I = 2bh^3/3$ the moment of inertia), (18) yields $S^{(2)}_{1313}$. In this computation we assumed the origin of the coordinate system at the cell's center, so that $S^{(2)}_{1313} = 2U^{*cell}/V$, whereby $U^{*cell} = U^{*couple-stress} = V\mu_{13} S^{(2)}_{1313} \mu_{13}/2$ with $\mu_{13} = M_B/Area$ ($Area = Lb\sqrt{3}/2$). Note that, in this case, the average couple-stress in the couple-stress medium $\tau_{11} = 0$. However, for other choices of coordinate system's origin, $\tau_{11} = \frac{1}{V}\int_V \sigma_{11} dV = \frac{1}{V}\int_{\partial B} \sigma_{11} n_1 x_1 dS$ will, in general, not vanish.

Deformation modes for these tests under traction boundary conditions are shown in Fig. 4. As mentioned above, in the bending test under traction boundary conditions, the coordinate system is chosen at the center of a unit cell.

4. COUPLE-STRESS MODULI: RESULTS AND DISCUSSION

As pointed out in Section 2, by varying the stiffness ratio E^i/E^m we can model a very wide spectrum of composite materials with either stiff or soft inclusions. Moreover, in the extreme cases of this ratio tending to very high or low numbers, we approach composites with rigid inclusions or pores, respectively; the actual values of ∞ or 0 cannot be set in our computational mechanics model. In the latter case, by raising the volume fraction of inclusions, we could arrive at the situation of cellular solids, which are essentially beam-network systems, Fig. 1(b). On the other hand, the case of inclusions of finite stiffness in a near-zero stiffness matrix would approach the setting of granular media, Fig. 1(c).

The choice of unit cells required to determine the couple-stress moduli is as follows: (i) for beam networks and systems with soft inclusions, the cell is centered at the beam connection nodes; (ii) for granular-type media, with soft matrix material, the unit cell is centered at the grain center. This leads to a rule of placement of unit cells in two-phase composite materials which is important for the curvature test (i.e., for tensor $C^{(2)}_{i3k3}$): *the unit cell should be centered in a stiffer phase*. As the stiffness ratio of two phases tends to 1, the unit cell's placement has an ever smaller effect, until in the physically singular case of no mismatch, it becomes immaterial. This special case is of no interest to us as here the material is homogeneous with no microstructure, and thus, is described by the classical elasticity theory. Summarizing, when the contrast is 1 - i.e., when both phases are identical - one should use an RVE at the scale much smaller than what we show in our figures 1-4. This new scale should be defined by the presence of another microscale - crystal lattice or molecular, say - and may also be Cosserat-type (e.g., Askar, 1986). Clearly, when the contrast is different from 1, the inclusions are present and we need to consider this new scale.

The complete computational mechanics procedure runs as follows:

i) For a given type of boundary conditions, the rhombus-shaped periodic unit cells of Figs. 1(b) and (c) are analyzed using the finite element software ABAQUS (1995), Figs. 2, 3, 4.

ii) Note that the equality $C^{(1)}_{1122} = C^{(1)}_{1111} - 2C^{(1)}_{1212}$, valid for isotropic media, which is only approximately satisfied for our case (within 3%), yields $C^{(1)}_{1122}$ directly. The same holds for compliances in case of the traction boundary condition.

iv) If the displacement or displacement-periodic conditions are being employed, compute, by inversion, the compliance components $S^{(1)}_{1111}$, $S^{(1)}_{1212}$, and $S^{(2)}_{1313}$.

v) Compute l from (3).

In Figs. 5, 6, 7 we present $C^{(1)}_{1111} \cong C^{(1)}_{2222}$, $C^{(1)}_{1212}$, and $C^{(2)}_{1313}$, respectively, obtained from each of three boundary conditions. They are plotted as functions of the stiffness ratio E^i/E^m, ranging from 10^{-4} through 10^4 for the matrix Poisson's ratio $\nu^m = 0.3$ and the inclusion Poisson's ratios $\nu^i = 0.3$, and are nondimensionalized by E^m. Note that the results of displacement-periodic boundary conditions always fall between those obtained by applying displacement and traction boundary conditions. Given the fact that γ_{ij} is symmetric, we can readily adapt the order relations formulated for apparent response tensors in classical elasticity (Hazanov and Huet, 1994)

$$\gamma_{ij}C^{(1)(tt)}_{ijkl}\gamma_{kl} \le \gamma_{ij}C^{(1)(dp)}_{ijkl}\gamma_{kl} \le \gamma_{ij}C^{(1)(dd)}_{ijkl}\gamma_{kl} \qquad \forall \gamma_{ij}, \gamma_{kl} \neq 0 \tag{19}$$

Here the superscripts denote three types of boundary conditions: *dd* -displacement, *dt*- traction, *tt*-traction. These give

$$\begin{gathered} C^{(1)(tt)}_{1111} \le C^{(1)(dp)}_{1111} \le C^{(1)(dd)}_{1111} \\ C^{(1)(tt)}_{1212} \le C^{(1)(dp)}_{1212} \le C^{(1)(dd)}_{1212} \\ C^{(1)(tt)}_{1111} - C^{(1)(tt)}_{1212} \le C^{(1)(dp)}_{1111} - C^{(1)(dp)}_{1212} \le C^{(1)(dd)}_{1111} - C^{(1)(dd)}_{1212} \end{gathered} \tag{20}$$

The last of these results is obtained under $\gamma_{11} = \gamma_{12}$, which makes it a most stringent condition; also, this presupposes the isotropy.

Next, we can adapt the same methodology as that leading to (19) to prove that the response tensors linking the curvature tensor with the couple-stress tensor follow the fully analogous order rela-

tions

$$\kappa_{i3} C^{(2)(tt)}_{i3k3} \kappa_{k3} \leq \kappa_{i3} C^{(2)(dp)}_{i3k3} \kappa_{k3} \leq \kappa_{i3} C^{(2)(dd)}_{i3k3} \kappa_{k3} \qquad \forall \kappa_{i3},\, \kappa_{k3} \neq 0 \qquad (21)$$

which implies

$$C^{(2)(tt)}_{i3k3} \leq C^{(2)(dp)}_{i3k3} \leq C^{(2)(dd)}_{i3k3} \qquad (22)$$

All these inequalities are satisfied; $(20)_{1,2}$ and (22) are given in Table 1, while $(20)_3$ can easily be obtained from this data.

It is interesting to note that we also find, by our computational mechanics study, the characteristic length l to exhibits this hierarchy (Fig. 8)

$$l^{(tt)} \leq l^{(dp)} \leq l^{(dd)} \qquad (23)$$

However, we do not have a mathematical proof of (21). Three plots in Fig. 8 show the characteristic lengths l, resulting from our three types of boundary conditions *tt*, *dp*, and *dd* - all nondimensionalized by the window size L (= 10 in our numerical study). While the right limit of E^i/E^m approximates the situation of rigid grains in the elastic matrix, the left limit approaches that of holes in the elastic matrix (porous material).

With respect to the latter case, we recall that the analytical, micropolar model of triangular beam networks (Wozniak, 1970) gives

$$l^{analytical} = \frac{L}{24} \frac{1 + 3\left(\frac{w}{L}\right)^2}{1 + \left(\frac{w}{L}\right)^2} \qquad (24)$$

This yields $\cong 0.21$ for beams of the width-to-length (w/L) ratio 1:4 or lower (i.e., from stubby to very slender). The optional correction owing to the Timoshenko, rather than Euler-Bernoulli, beam formulation is negligible. According to Fig. 8, the value 0.21 is clearly bounded (!), respectively from above and below, by the results of tests conducted under displacement and traction boundary

conditions, that is

$$l^{(tt)} < l^{analytical} \leq l^{(dd)} \tag{25}$$

Inequality (23) shows that the l's we obtained from traction and displacement boundary conditions of the couple-stress theory bound $l^{analytical}$ resulting from the more correct (and better posed) micropolar theory (Eringen, 1999). Moreover, we note that the displacement-periodic boundary conditions do consistently give $l^{analytical} < l^{(dp)} < l^{(dd)}$ for the entire range of E^i/E^m.

It is important to note two more things here:

(a) The characteristic length l is on the same order for the entire ranges of E^i/E^m; in (Ostoja-Starzewski, *et al.*, 1999) it was also found to be the case for three different volume fractions; it changes most dramatically for E^i/E^m ranging from 10^{-2} to 10^2.

(b) As already mentioned earlier in this paper, the particular case of E^i/E^m being exactly unity corresponds to a physically singular situation of a homogeneous medium of the Cauchy type - the same as that of which both classical elastic phases are being made - for which no Cosserat approximation is necessary.

Finally, the calculated data for the three stiffness constants $C^{(1)}_{1111}$ (or $C^{(1)}_{2222}$), $C^{(1)}_{1212}$, and $C^{(2)}_{1313}$, and corresponding characteristic lengths l are also given in Table 1. Here we include the results calculated by displacement (*dd*), displacement-periodic (*dp*) and traction (*tt*) boundary conditions, obtained in this paper and shown in Figs. 5-8, and include for comparison, in the last column, those for $C^{(1)}_{1111}$ and $C^{(1)}_{1212}$ calculated from periodic boundary conditions (*pp*), reported in Ostoja-Starzewski *et al.* (1999). Note that the stiffnesses obtained by periodic boundary conditions are also bounded by those calculated by using displacement and traction boundary conditions. The data given in the last column corrects an error which we found in our earlier paper (Ostoja-Starzewski *et al.*, 1999). Namely, a factor 1/2 was accidentally omitted there in the energy expression in calculation of $C^{(2)}_{1313}$; this resulted in a reported characteristic length smaller by a factor of $\sqrt{2}$. Note that the characteristic length obtained by using periodic/displacement-periodic (*pp* & *dp*)

boundary conditions is not bounded anymore by the displacement boundary conditions.

Acknowledgment

Support by the NSF under grants CMS-9713764 and CMS-9753075 is gratefully acknowledged.

References

ABAQUS (1995), Version 5.6, Hibbit, Karlsson & Sorensen, Inc. USA.

Askar, A. (1986), *Lattice Dynamical Foundations of Continuum Theories*, World Scientific, Singapore.

Bazant, Z.P. and Christensen, M. (1972), Analogy between micropolar continuum and grid frameworks under initial stress, *Int. J. Solids Structures* **8**, 327-346.

Cosserat, E. and F. (1909), *Théorie des Corps Déformables*, A. Herman et Fils, Paris.

Eringen, A.C. (1999), *Microcontinuum Field Theories I. Foundations and Solids*, Springer-Verlag.

Forest, S. and Sab, K. (1998), Cosserat overall modeling of heterogeneous materials, *Mech. Res. Comm.* **25**(4), 449-454.

Hazanov, S. and Huet, C. (1994), Order relationships for boundary conditions effect in the heterogeneous bodies smaller than the representative volume, *J. Mech. Phys. Solids* **42**, 1995-2011.

Herrmann, G. and Achenbach, J.D. (1968), Applications of theories of generalized Cosserat continua to the dynamics of composite materials, in E. Kröner (ed.), *Mechanics of Generalized Continua*, Proc. IUTAM Symposium, 69-79, Springer Verlag, Berlin.

Jiang, M., Alzebdeh, K., Jasiuk, I. and Ostoja-Starzewski, M. (2000), Scale and boundary conditions effects in elasticity of random composites, *Acta Mechanica,* in press.

Lakes, R.S. (1983), Size effects and micromechanics of a porous solid, *J. Mat. Sci.* **18**, 2572-2580.

Lakes, R.S. (1986), Experimental microelasticity of two porous solids, *Int. J. Solids Structures* **22**, 55-63.

Lakes, R. (1995), Experimental methods for study of Cosserat elastic solids and other generalized elastic continua, in H.-B. Mühlhaus (ed.), *Continuum Models for Materials with Microstructure*, 1-25, Chichester: John Willey & Sons.

Nowacki, W. (1986), *Theory of Asymmetric Elasticity*, Oxford, Pergamon Press/Warsaw, Polish Scientific Publishers.

Nowacki, W. (1986), *Advances in Theory of Elasticity* (in Polish), Polish Scientific Publishers, Warsaw.

Ostoja-Starzewski, M., Boccara, S. and Jasiuk, S. (1999), Couple-stress moduli and characteristic length of composite materials, *Mech. Res. Comm.* **26**(4), 387-397.

Ostoja-Starzewski, M. and Jasiuk, I. (1995), Stress invariance in planar Cosserat elasticity, *Proc. Roy. Soc. Lond. A* **451**, 453-470.

Perkins, R.W. and Thomson, D. (1973), Experimental evidence of a couple-stress effect, *AIAA J.* **11**, 1053-1055.

Sanchez-Palencia, E. and Zaoui, A. (eds.) (1987), *Homogenization Techniques for Composite Media*, Lecture Notes in Physics **272**.

Wozniak, C. (1970), *Surface Lattice Structures* (in Polish), Polish Scientific Publishers, Warsaw.

Yang, J. F. C. and Lakes, R. S. (1982), Experimental study of micropolar and couple-stress elasticity in bone in bending, *J. Biomechanics*, **15**, 91-98.

Table

Table 1. $C^{(1)}_{1111}$ (or $C^{(1)}_{2222}$), $C^{(1)}_{1212}$, and $C^{(2)}_{1313}$, non-dimensionalized by E^m, and the corresponding characteristic lengths l, nondimensionalized by L, obtained by four different boundary conditions: displacement (*dd*), displacement-periodic (*dp*), periodic (*pp*), and traction (*tt*) for E^i/E^m ranging from 10^{-4} to 10^4 and $\nu = 0.3$ for volume fraction 18.4 %. The columns *dd* and *dp* give $C^{(1)}_{2222}$, while *tt* gives $C^{(1)}_{1111}$ obtained by inversion of the $S^{(1)}_{ijkl}$ tensor.

Figure Legends

Fig. 1(a) A periodic, globally isotropic, matrix-inclusion composite, of period L, with inclusions of diameter d; (b) a periodic unit cell with an inclusion at the corner; (c) a periodic unit cell with an inclusion at the center.

Fig. 2. Tests for the determination of couple-stress constants $C^{(1)}_{2222}$, $C^{(1)}_{1212}$, and $C^{(2)}_{1313}$ under displacement boundary conditions. Left (right) column corresponds to the inclusion at the corner (center).

Fig. 3. Tests for the determination of constants $C^{(1)}_{2222}$, $C^{(1)}_{1212}$, and $C^{(2)}_{1313}$ under displacement-periodic boundary conditions. Left (right) column corresponds to the inclusion at the corner (center).

Fig. 4. Tests for the determination of constants $S^{(1)}_{2222}$, $S^{(1)}_{1212}$, and $S^{(2)}_{1313}$ under displacement boundary conditions. Left (right) column corresponds to the inclusion at the corner (center).

Fig. 5. The effective moduli $C^{(1)}_{1111} = C^{(1)}_{2222}$, non-dimensionalized by E^m, from three types of boundary conditions (displacement (dd), displacement-periodic (dp), and traction (tt)) plotted as functions of the stiffness ratio E^i/E^m for the case of the Poisson's ratio $\nu^m = \nu^i = 0.3$ at volume fraction 18.4%.

Fig. 6. The effective moduli $C^{(1)}_{1212}$, non-dimensionalized by E^m, from three types of boundary conditions plotted as functions of the stiffness ratio E^i/E^m for the case of the Poisson's ratio $\nu^m = \nu^i = 0.3$ at volume fraction 18.4%.

Fig. 7. The effective moduli $C^{(2)}_{1313}$, non-dimensionalized by E^m, from three types of boundary conditions plotted as functions of the stiffness ratio E^i/E^m for the case of the Poisson's ratio $\nu^m = \nu^i = 0.3$ at volume fraction 18.4%.

Fig. 8. The characteristic length l, non-dimensionalized by the unit cell size L, as a function of the stiffness ratio E^i/E^m, computed from the results of Figs. 5-7. Cases of three boundary conditions are shown.

Isotropic cell 10*8.66 (Em=1)

		dd	dp	tt	pp
C1111	Ei/Em=0.0001	0.7284	0.6641	0.0008	0.6627
	Ei/Em=0.001	0.7291	0.6650	0.0083	0.6636
	Ei/Em=0.01	0.7359	0.6734	0.0774	0.6721
	Ei/Em=0.1	0.7968	0.7483	0.4747	0.7474
	Ei/Em=10	1.4419	1.4396	1.3860	1.4088
	Ei/Em=100	1.5135	1.5096	1.4284	1.4673
	Ei/Em=1000	1.5212	1.5173	1.4363	1.4734
	Ei/Em=10000	1.5210	1.5181	1.4362	1.4742

		dd	dp	tt	pp
C1212	Ei/Em=0.0001	0.2722	0.2534	0.0004	0.2273
	Ei/Em=0.001	0.2724	0.2537	0.0035	0.2276
	Ei/Em=0.01	0.2744	0.2560	0.0320	0.2306
	Ei/Em=0.1	0.2914	0.2773	0.1767	0.2586
	Ei/Em=10	0.5062	0.4924	0.4733	0.4911
	Ei/Em=100	0.5316	0.5121	0.4864	0.5107
	Ei/Em=1000	0.5345	0.5142	0.4877	0.5128
	Ei/Em=10000	0.5348	0.5145	0.4878	0.5129

		dd	dp	tt	dp
C1313	Ei/Em=0.0001	7.1181	5.8859	0.0024	5.8859
	Ei/Em=0.001	7.1238	5.8971	0.0244	5.8971
	Ei/Em=0.01	7.1902	5.9935	0.2341	5.9935
	Ei/Em=0.1	7.8198	6.8662	1.7429	6.8662
	Ei/Em=10	13.4685	13.3227	6.6527	13.3227
	Ei/Em=100	13.8245	13.7118	6.7712	13.7118
	Ei/Em=1000	13.8702	13.7561	6.7856	13.7561
	Ei/Em=10000	13.8748	13.7607	6.7856	13.7607

		dd	dp	tt	pp & dp
characteristic length	Ei/Em=0.0001	0.2557	0.2410	0.1314	0.2544
	Ei/Em=0.001	0.2557	0.2407	0.1318	0.2545
	Ei/Em=0.01	0.2560	0.2415	0.1352	0.2549
	Ei/Em=0.1	0.2590	0.2486	0.1570	0.2576
	Ei/Em=10	0.2579	0.2559	0.1875	0.2604
	Ei/Em=100	0.2550	0.2531	0.1866	0.2591
	Ei/Em=1000	0.2547	0.2527	0.1865	0.2590
	Ei/Em=10000	0.2547	0.2527	0.1865	0.2590

Table 1

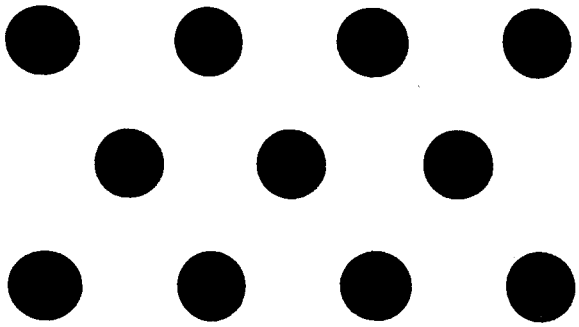

(a)

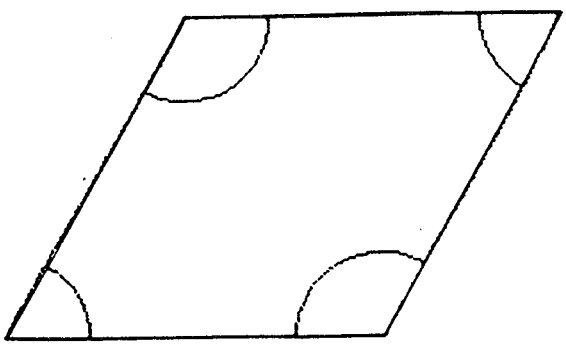

(b)

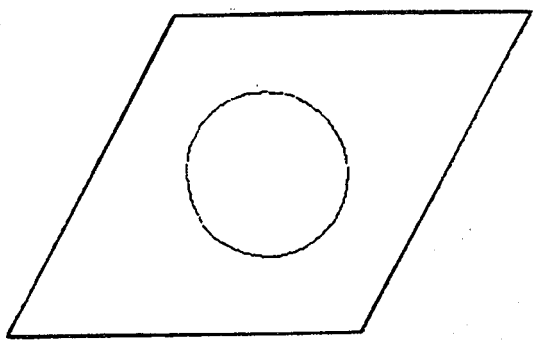

(c)

Figure 1

Deformed shapes. Displacement boundary conditions.

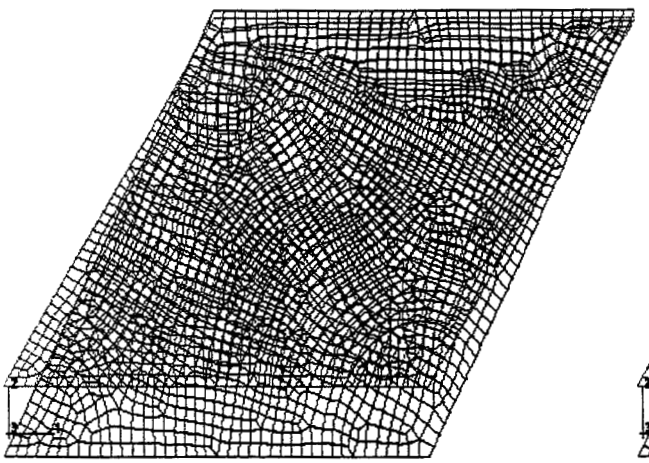

C^1_{2222}

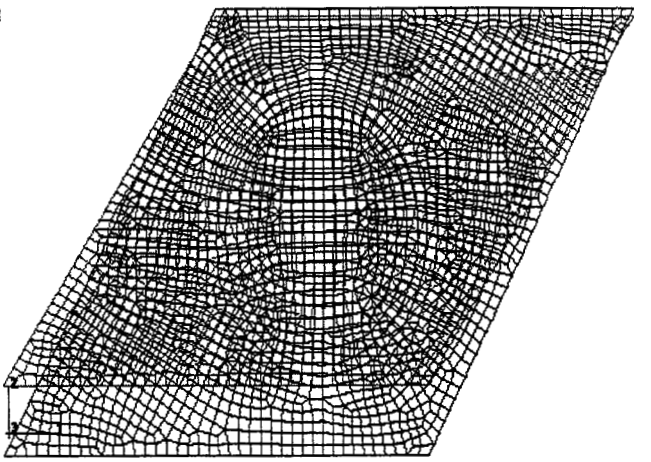

C^1_{2222}

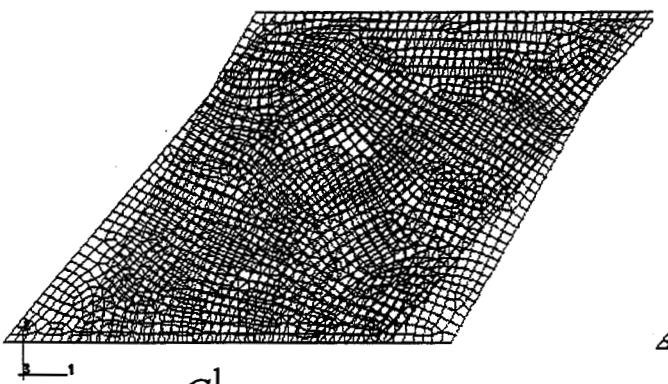

C^1_{1212}

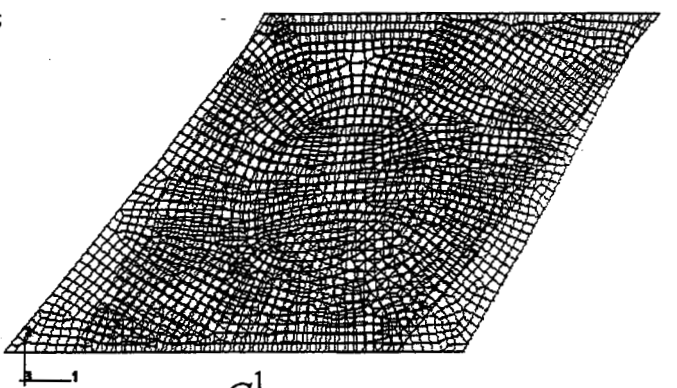

C^1_{1212}

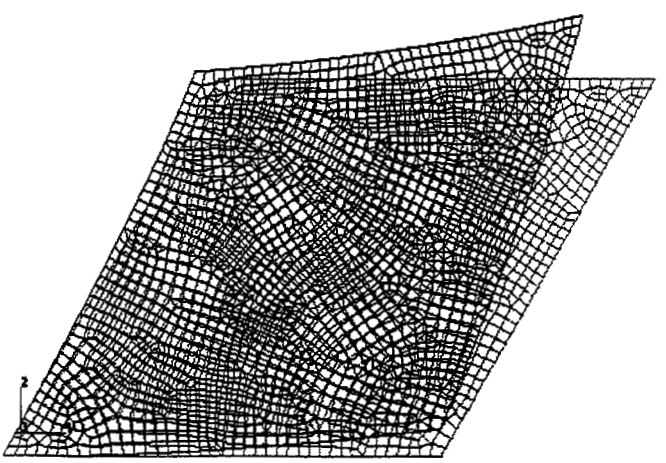

C^2_{1313}

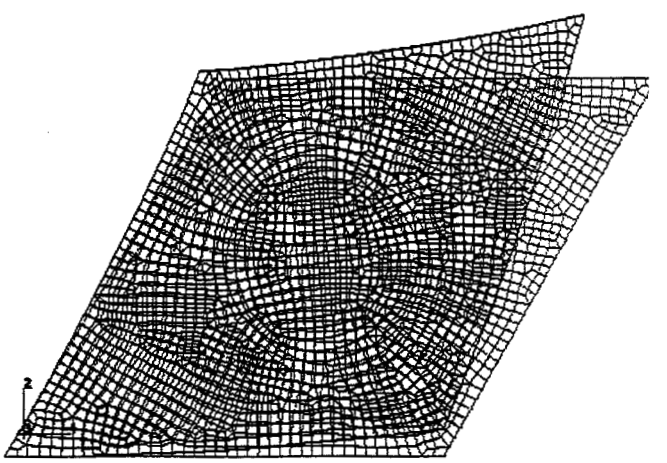

C^2_{1313}

Deformed shapes. Displacement-Periodic boundary conditions.

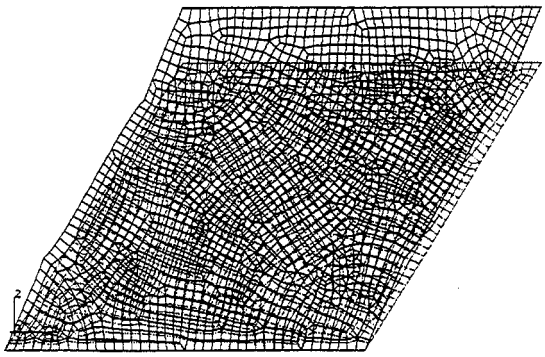

C^1_{2222}

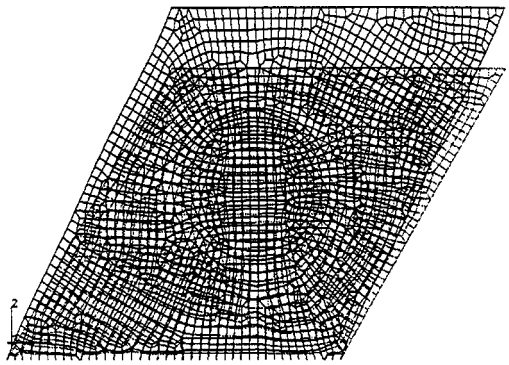

C^1_{2222}

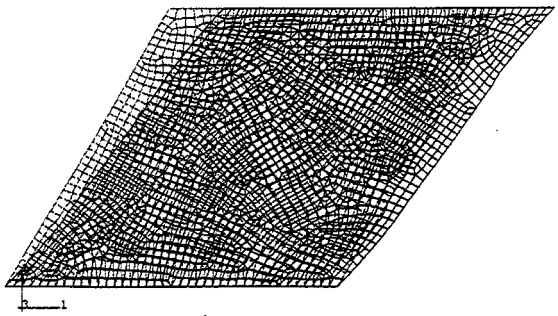

C^1_{1212}

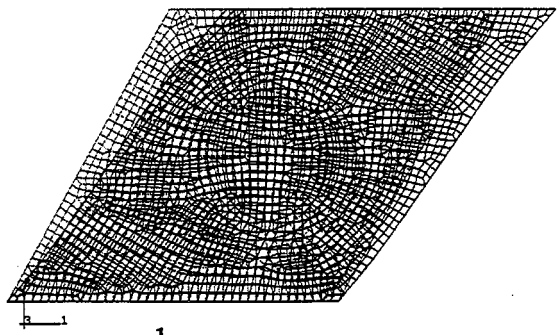

C^1_{1212}

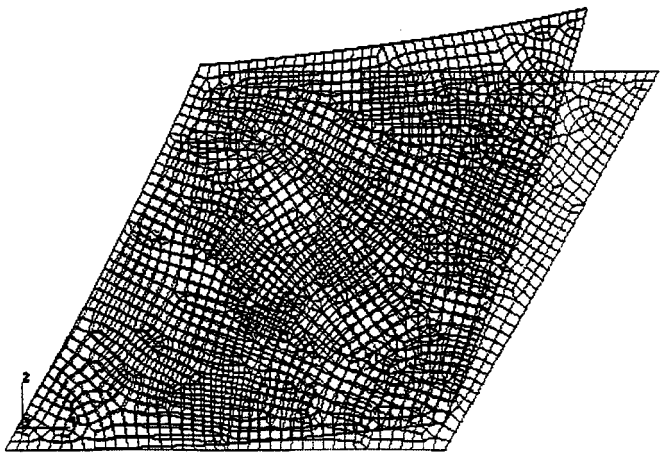

C^2_{1313}

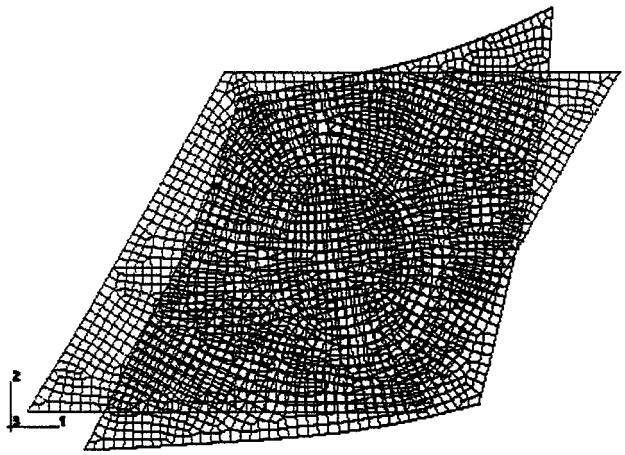

C^2_{1313}

Deformed shapes. Traction boundary conditions.

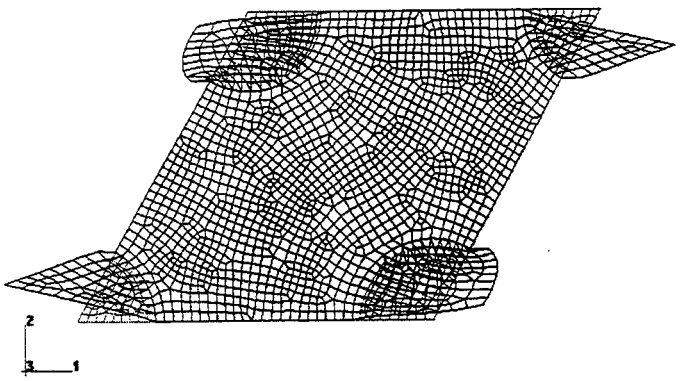

S^1_{2222}

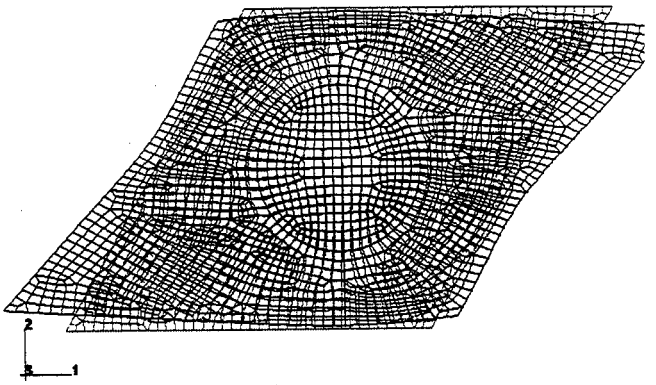

S^1_{2222}

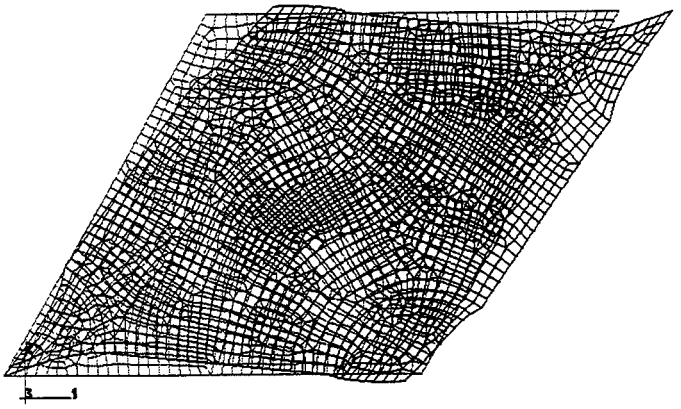

S^1_{1212}

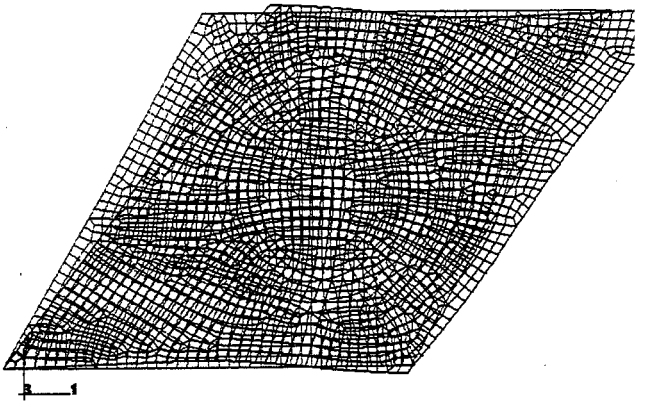

S^1_{1212}

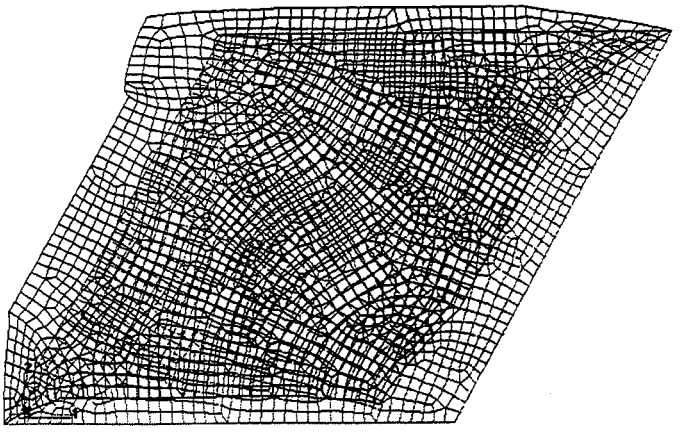

S^2_{1313}

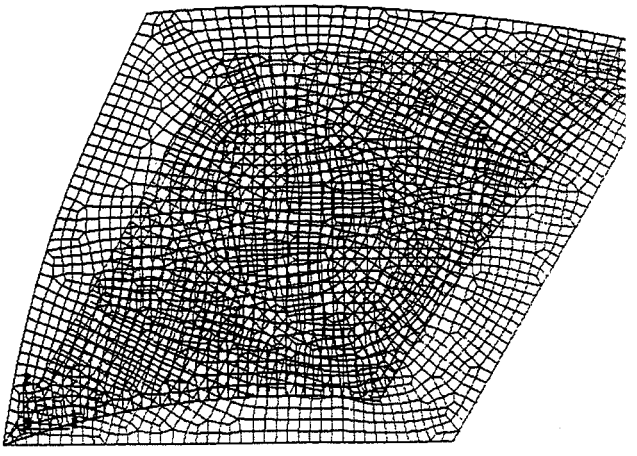

S^2_{1313}

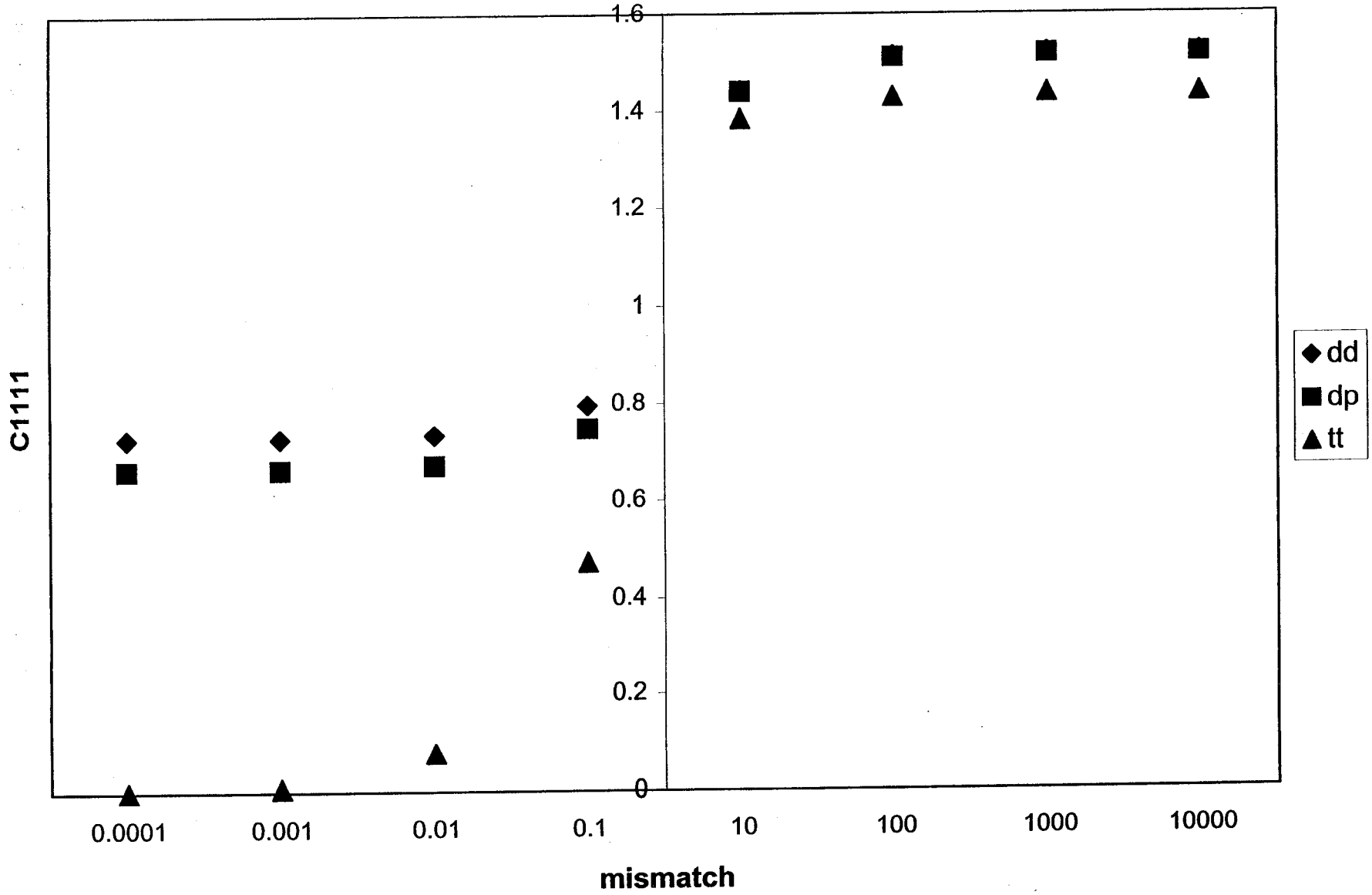
C1111
1.6
1.4
1.2
1
0.8
0.6
0.4
0.2
0
0.0001
0.001
0.01
0.1
10
100
1000
10000
mismatch
dd
dp
tt

Figure 5

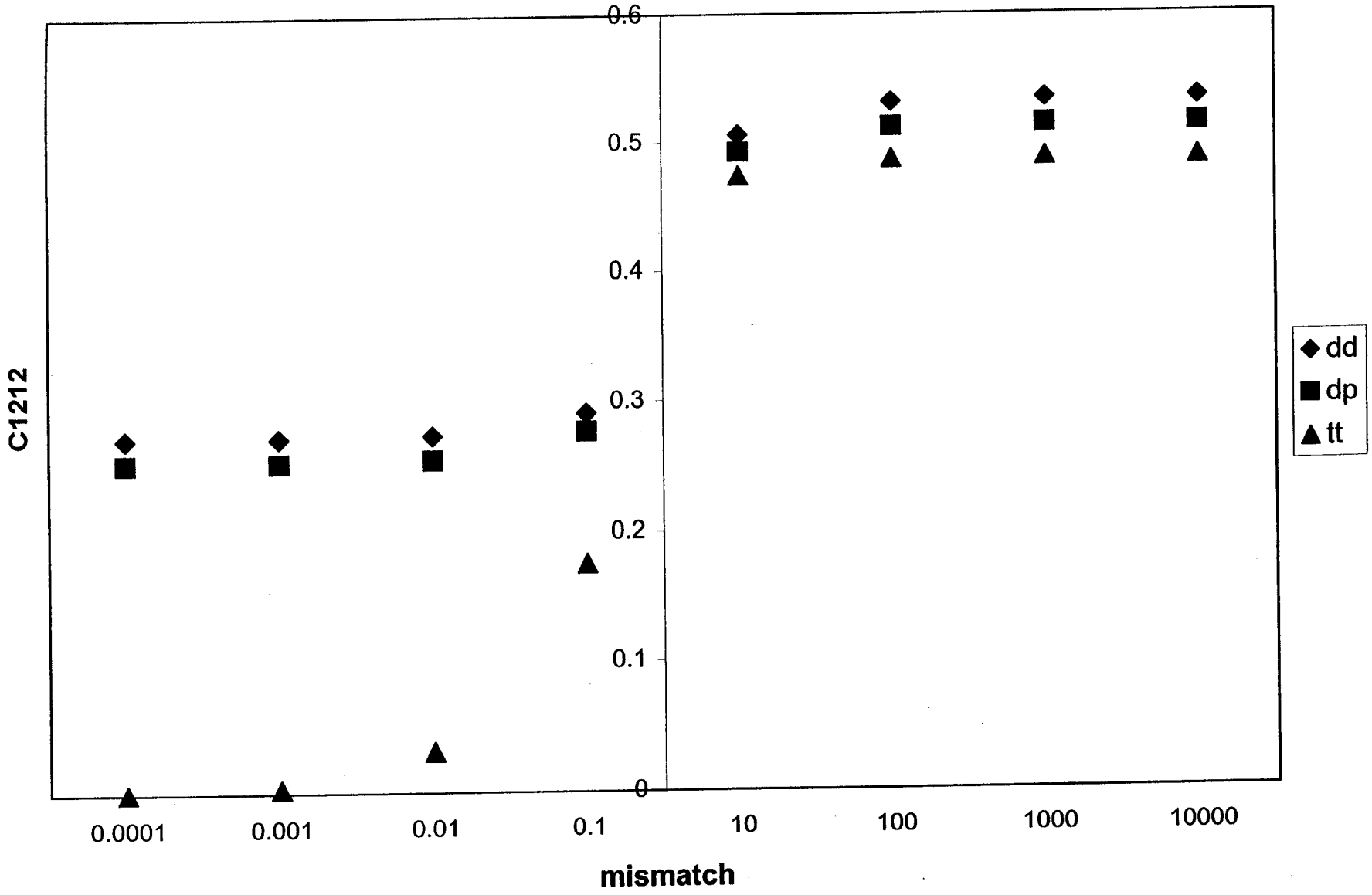
C1212
0.6
0.5
0.4
0.3
0.2
0.1
0
0.0001
0.001
0.01
0.1
10
100
1000
10000
mismatch
dd
dp
tt

Figure 6

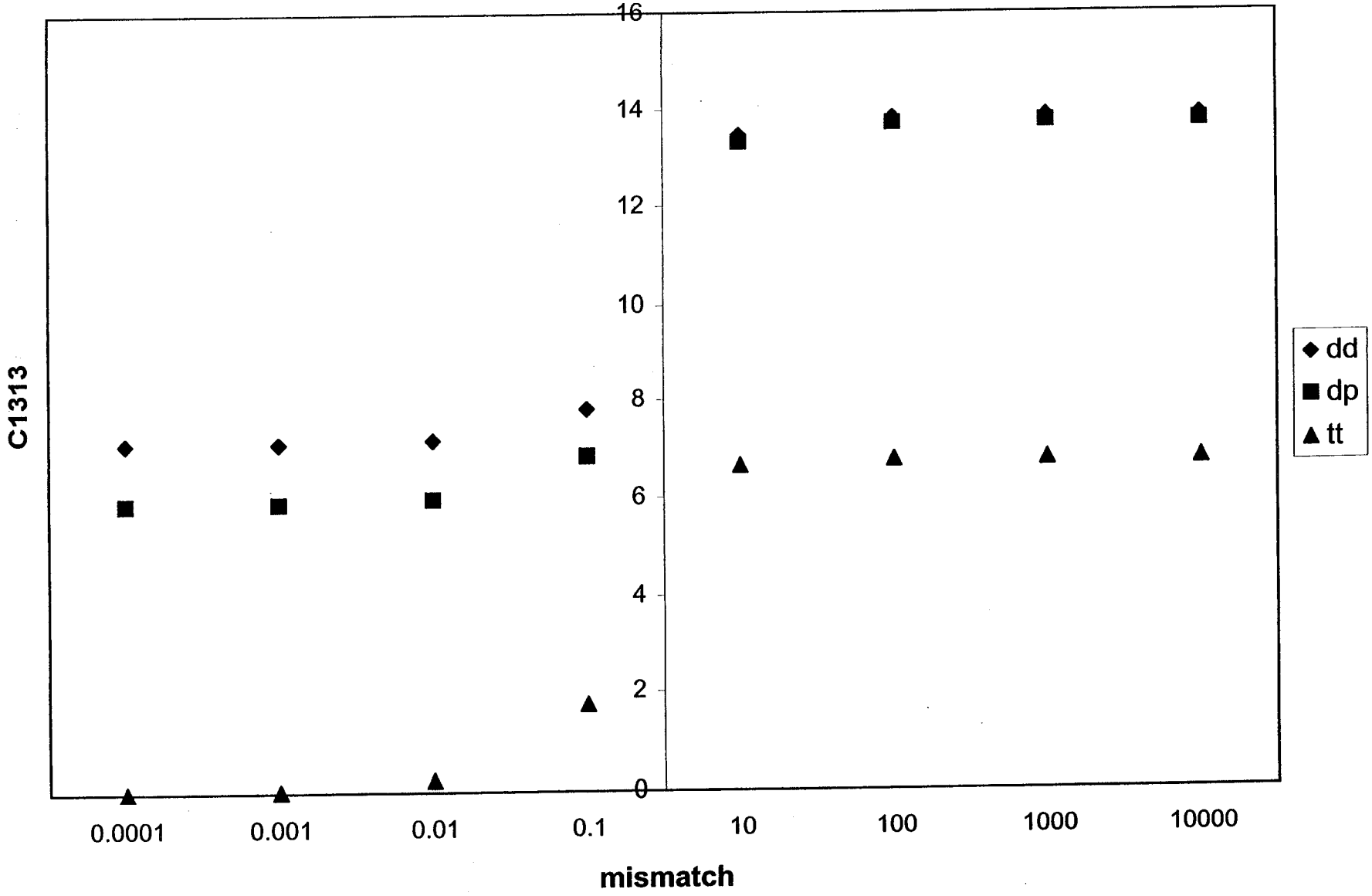
C1313
16
14
12
10
8
6
4
2
0
0.0001
0.001
0.01
0.1
10
100
1000
10000
mismatch
dd
dp
tt

Figure 7

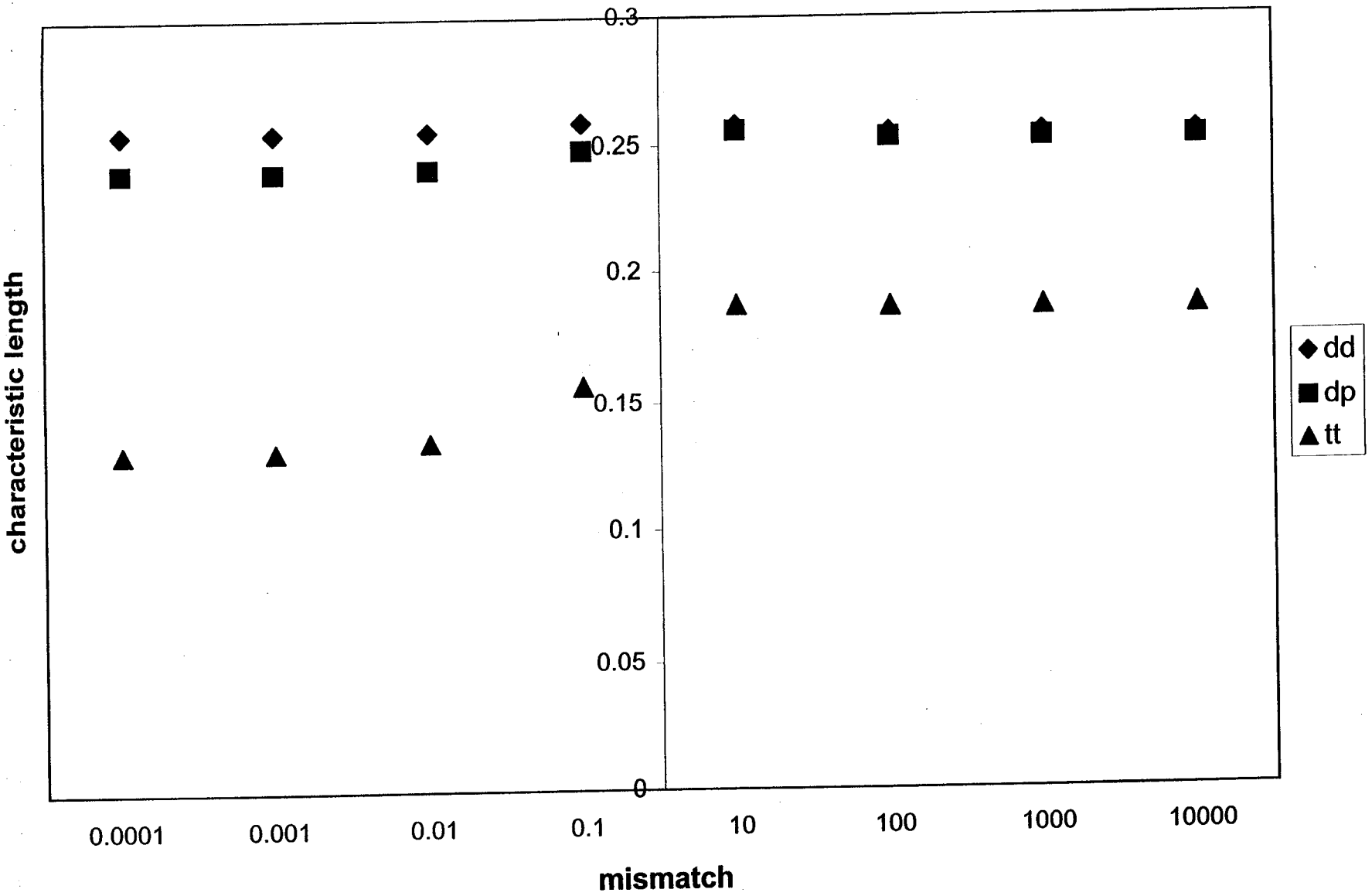
0.3
0.25
0.2
0.15
0.1
0.05
0
characteristic length
0.0001
0.001
0.01
0.1
10
100
1000
10000
mismatch
dd
dp
tt

Figure 8